Downconversion for solar cells in $NaYF_4:Er,Yb$

L. Aarts,[a] B. M. van der Ende, and A. Meijerink
Condensed Matter and Interfaces, Debye Institute for Nanomaterials Science, Utrecht University, Princetonplein 5, 3584 CC Utrecht, The Netherlands

(Received 8 April 2009; accepted 19 June 2009; published online 24 July 2009)

Downconversion is a promising avenue to boost the efficiency of solar cells by absorbing *one* higher energy visible photon and emitting *two* lower energy near-infrared (NIR) photons. Here the efficiency of downconversion for the (Er^{3+}, Yb^{3+}) couple is investigated in $NaYF_4$, a well-known host lattice for efficient upconversion with (Er^{3+}, Yb^{3+}). Analysis of the excitation and emission spectra for $NaYF_4$ doped with 1% Er^{3+} and codoped with 0%, 5%, 10%, or 30% Yb^{3+} show that visible to NIR downconversion is inefficient. Downconversion by the scheme based on the reverse of the upconversion process is hampered by fast multiphonon relaxation from the $^4F_{7/2}$ level (the starting level for downconversion) to the $^4S_{3/2}$ level. Energy transfer from the $^4S_{3/2}$ level of Er^{3+} to Yb^{3+} is shown to be inefficient. Efficient downconversion from the $^4G_{11/2}$ of Er^{3+} level is observed, resulting in emission of two photons (one around 980 nm and one around 650 nm) after absorption of a single 380 nm photon. © *2009 American Institute of Physics*. [DOI: 10.1063/1.3177257]

I. INTRODUCTION

A large part of the energy losses that limit the conversion efficiency of solar cells to 30% is related to the spectral mismatch.[1] Photons with an energy smaller than the band gap (E_g) will not be absorbed (subband-gap transmission) and a large part of the energy of photons with an energy larger than the band gap is lost as heat (thermalization losses). The energy losses related to the spectral mismatch can be reduced by adapting the solar cells by combining multiple semiconductor materials with different band gaps, each converting a different part of the solar spectrum with high efficiency. This approach has been successfully applied and energy efficiencies over 40% have been reported.[2] An alternative way to reduce the spectral mismatch losses is through adapting the solar spectrum so that the solar cell can use it more efficiently.

There are two options to adapt the solar spectrum. The first option is to add two lower energy photons (that are transmitted) to obtain one higher energy photon that can be absorbed by the solar cell. This process is known as upconversion (UC) and is especially useful for solar cells with a large band gap where transmission losses dominate. The second way to adapt the solar spectrum is to split one higher energy photon to obtain two photons with a smaller energy. Each of these photons can subsequently be absorbed by the solar cell and generate an electron-hole pair. This is known as downconversion (DC) and is most beneficial for solar cells with a smaller band gap where thermalization losses are the major loss factor. Because one photon is "cut" into two smaller energy photons this process is also known as quantum cutting. The lanthanide ions are very well suited to use for DC or UC because they have a rich energy level structure that allows for efficient spectral conversion. There are many examples of efficient UC and DC using lanthanides, either with one type of lanthanide ion or a pair of lanthanide ions.[3,4]

Trupke *et al.*[5–7] have performed extensive calculations to determine the effect of using either UC or DC materials in combination with solar cells. With an ideal downconverter material (splitting every photon above 2 E_g into two photons that both can be absorbed) a limit of efficiency of 40% is possible for a solar cell with a band gap of 1.1 eV.[5] Combining a ~2 eV solar cell with an ideal upconverter can raise the upper limit of the conversion efficiency to ~50%.[6,7] An important issue in the case of UC materials is that UC is a nonlinear process: for the two step UC process (where two photons are added to obtain one photon with a larger energy) the UC light intensity I_{UC} is proportional to square of the incident light intensity I_i. Therefore high conversion efficiencies are only obtained at sufficiently high excitation density which can be easily realized using lasers, but will require strong concentration of sunlight. The most efficient UC is realized using lanthanide ions.[3] An example of a particularly efficient upconverting couple is Er^{3+} and Yb^{3+}. Under high power laser excitation an efficiency of around 50% has been reported for the conversion of NIR (~1000 nm) to visible light in $NaYF_4:Er^{3+},Yb^{3+}$.[8] Another example is near-infrared (NIR) UC by $NaYF_4$ doped with Er^{3+}, which was applied to the rear of a silicon solar cell and shown to convert 1400–1500 nm NIR to photons that can be absorbed by the *c*-Si solar cell.[7,9]

Contrary to UC, DC is a linear process. This makes it possible to obtain high conversion efficiencies, independent of the incident power and allows for the use of nonconcentrated sunlight. Compared to the UC materials, demonstrations of efficient DC materials are limited. The (Gd^{3+}, Eu^{3+}) couple in a $LiGdF_4$ host lattice shows efficient DC (internal quantum efficiency of approximately 190%) and Er^{3+}, Gd^{3+} and Tb^{3+} in the same host lattice have an efficiency of 130%.[4,10,11] Both of these are examples of systems where DC of VUV photons into two visible photons take place.

DC of UV or visible photons into NIR photons was first demonstrated in $(Y,Yb)PO_4:Tb^{3+}$.[12] After excitation into the $^5D_4$ state of the Tb^{3+} ion two neighboring Yb^{3+} ions are

[a]Electronic mail: l.aarts@uu.nl.

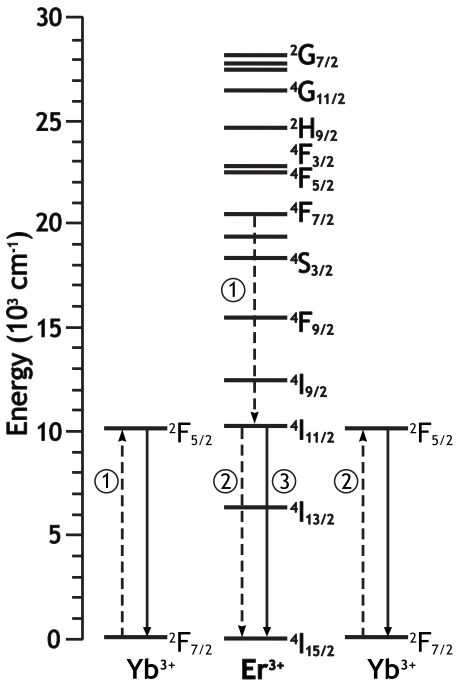

FIG. 1. Energy level schemes of the Er^{3+} ($4f^{11}$) and Yb^{3+} ($4f^{13}$) couple showing two possible mechanisms for DC. First energy is transferred from Er^{3+} to one Yb^{3+} neighbor [1: Er^{3+} ($^4F_{7/2} \rightarrow {}^4I_{11/2}$) and Yb^{3+} ($^2F_{7/2} \rightarrow {}^2F_{5/2}$)] followed by emission of an infrared photon by Yb^{3+} ($^2F_{5/2} \rightarrow {}^2F_{7/2}$). The remaining energy can either be transferred to a second Yb^{3+} neighbor [2: Er^{3+} ($^4I_{11/2} \rightarrow {}^4I_{15/2}$) and Yb^{3+} ($^2F_{7/2} \rightarrow {}^2F_{5/2}$)], or emitted by Er^{3+} (3: $^4I_{11/2} \rightarrow {}^4I_{15/2}$).

excited through a cooperative energy transfer process. The $^5D_4$ level of Tb^{3+} is situated at about twice the energy of the Yb^{3+} $^2F_{7/2}$ level, and after energy transfer Yb^{3+} emission is observed around 1000 nm. This is just above the band gap of crystalline silicon which makes Yb^{3+} an attractive candidate for DC materials to be used in combination with *c*-Si solar cells. More recently, cooperative DC has also been reported for (Tb^{3+}, Yb^{3+}) [13,14] and other lanthanide couples, viz. (Pr^{3+}, Yb^{3+})[15] and (Tm^{3+}, Yb^{3+}).[16] However, it is not clear that the second-order cooperative energy transfer process is the operative mechanism in the latter two systems, as first-order energy transfer processes are also possible, and are expected to dominate.[17] The lower efficiency of second-order cooperative energy transfer process makes it only efficient at very high Yb^{3+} concentrations where the Yb^{3+} emission is largely quenched through concentration quenching. To achieve more efficient energy transfer, an intermediate level on the donor ion should be used in order to obtain DC through two resonant energy transfer steps.

In this paper we investigate if efficient DC is possible with the Er^{3+}, Yb^{3+} couple. In the past it has been shown that Er^{3+} and Yb^{3+} is a particularly efficient upconverting couple.[8] We have chosen $NaYF_4$ as a host lattice to study DC since this host is well known for efficient UC by Yb^{3+},Er^{3+} and the host lattice has a small phonon energy (maximum phonon energy ~400 cm^{-1}). A low phonon energy is crucial: in Fig. 1 the DC scheme for the Er^{3+},Yb^{3+} couple is shown. It is the reverse of the well-known UC scheme. In the first step energy transfer from the $^4F_{7/2}$ level of Er^{3+} occurs: Er^{3+} ($^4F_{7/2} \rightarrow {}^4I_{11/2}$) and Yb^{3+} ($^2F_{7/2} \rightarrow {}^2F_{5/2}$) thus populating the $^2F_{5/2}$ level of Yb^{3+}. In the second step energy transfer to a second Yb^{3+} ion can occur from the $^4I_{11/2}$ level of Er^{3+} while it is also possible that Er^{3+} emits a photon around 1000 nm from the $^4I_{11/2}$ level. In order to have efficient DC it is crucial to prevent (fast) nonradiative decay from the $^4F_{7/2}$ level to the $^4S_{3/2}$ level since DC from the $^4S_{3/2}$ level is not possible. Since nonradiative relaxation from the $^4F_{7/2}$ level is determined by multiphonon relaxation, a low phonon energy is required to reduce the multiphonon relaxation rate. In this paper we will show that DC from the $^4F_{7/2}$ level cannot compete with multiphonon relaxation from this level and that host lattices with a lower phonon energy are required. However, from the higher energy $^4G_{11/2}$ level, DC is observed.

II. METHODS

Powder samples of $NaYF_4$ doped with Er^{3+} and Yb^{3+} were prepared by a dry mixture method. NaF (Merck, p.a., 5% excess) was mixed with YF_3 (Chempur, 5*N*), ErF_3 (Highways, 3*N*), and YbF_3 (Chempur, 4*N*). The blend was then put into an alumina crucible and fired in an oven together with an excess of NH_4F (Sigma-Aldrich, 98+%) under a nitrogen flow. The samples were first heated to 300 °C for 2 h and then to 550 °C for 3 h. After the samples had cooled sufficiently they were crushed with a pestle and mortar and x-ray diffraction measurements were performed to check for phase purity.

Diffuse reflectance spectra were measured with a Perkin-Elmer Lambda 950 UV/VIS/IR absorption spectrometer. Emission and excitation spectra were measured with a SPEX DM3000F spectrofluorometer with a 450 W Xe lamp as the excitation source. Excitation and emission wavelengths were selected with a double-grating 0.220 m SPEX 1680 monochromator (1200 l/mm) blazed at 300 nm. Emission spectra were recorded by focusing the emitted light on a fiber guiding the light to a 0.3 m monochromator (Scientific Spectra Pro, Princeton Instruments) where the emission light is dispersed by a 150 l/mm grating or a 1200 l/mm grating, both blazed at 500 nm. The dispersed light was detected with a Princeton Instruments 300i charge coupled device. The SPEX spectrofluorometer is equipped with an Oxford helium flow cryostat for low temperature measurements. The spectra were not corrected for the instrumental response.

Lifetime measurements with an excitation wavelength of 380 nm were performed with a Lambda Physik LPD3000 tunable dye laser using a BIBUQ dye solution (tunable between 367–405 nm). The dye laser is pumped by a Lambda Physik LPX100 excimer (XeCl) laser. The typical pulse width for the setup is ~20 ns and the repetition rate is 10 Hz.

III. RESULTS AND DISCUSSIONS

Samples of $NaYF_4$ doped with 1 mol % Er^{3+} and 0, 5, 10, and 30 mol % Yb^{3+} and one sample doped with 5 mol % Yb^{3+} and no Er^{3+} were synthesized. X-ray diffraction measurements gave similar results for all five samples. They consist mostly of the hexagonal β crystal phase, although trace amounts of the cubic α phase of $NaYF_4$ are also

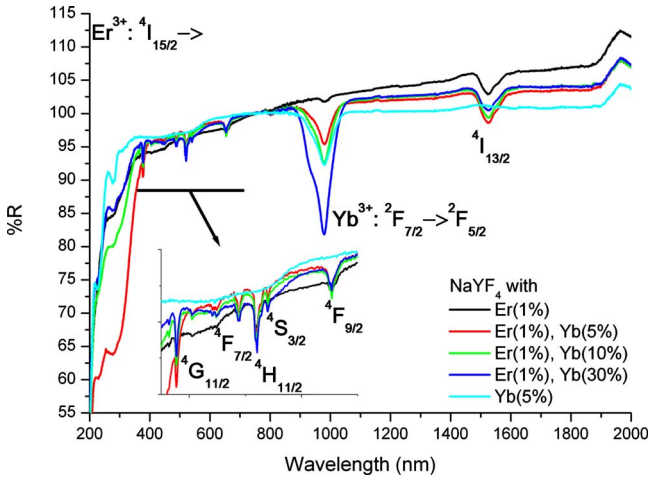

FIG. 2. (Color online) Diffuse reflectance spectra for $NaYF_4:Er^{3+}$ (1%), Yb^{3+} (0%, 5%, 10%, and 30%), and $NaYF_4:Yb^{3+}$ (5%).

present. The hexagonal β crystal phase has been shown to be the more efficient of the two crystal phases for UC.[18]

In the diffuse reflectance spectra (Fig. 2) it can be seen that the absorption strengths for the peaks corresponding to Er^{3+} transitions (e.g., the $^4I_{15/2} \rightarrow {}^4F_{7/2}$ transition around 500 nm and the $^4I_{15/2} \rightarrow {}^4I_{13/2}$ transition around 1550 nm) are the same for all samples that were doped with Er^{3+}. This means that the Er^{3+} concentration incorporated in the various samples is similar, as expected on the same amounts of Er^{3+} (1 mol %) present in the starting mixture. The absorption strength of the peak for the Yb^{3+} absorption around 1000 nm varies according to the Yb^{3+} concentration present in the starting mixtures. In the UV range an absorption band between 200 and 400 nm is observed which is probably related to defects, possibly involving oxygen impurities. The band is strongest for the sample codoped with 1% Er^{3+} and 5% Yb^{3+}.

In Fig. 3 the emission spectra of $NaYF_4:Er^{3+}$ (1%) and Yb^{3+} (0%, 5%, 10%, and 30%) are shown. The spectra were measured under identical conditions so that the intensities of the emissions may be compared. In the sample doped with Er^{3+} only, excitation in the Er^{3+} $^4F_{5/2}$ (451 nm) level yields

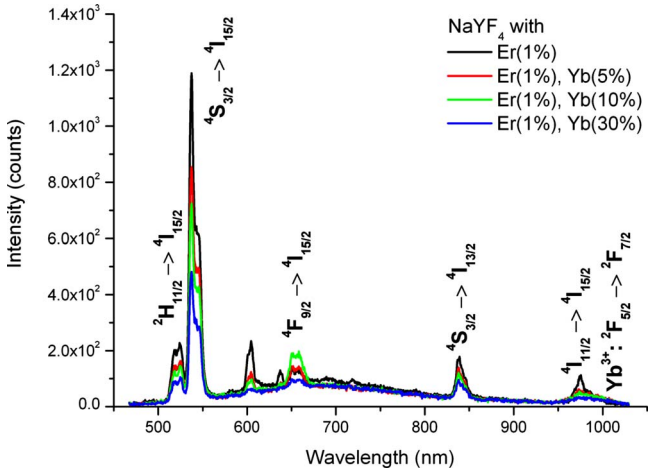

FIG. 3. (Color online) Room temperature emission spectra of $NaYF_4:Er^{3+}$ (1%) and Yb^{3+} (0%, 5%, 10%, and 30%). The excitation wavelength is 451 nm ($^4F_{5/2}$ level).

emission from the $^4S_{3/2}$, $^4F_{9/2}$, and $^4I_{11/2}$ levels, but no emission from the $^4F_{7/2}$ level is observed. This shows that nonradiative relaxation from the $^4F_{7/2}$ to the next lower level ($^2H_{11/2}$) is fast and radiative decay from the $^4F_{7/2}$ level cannot compete with nonradiative relaxation. The intensity of the Er^{3+} emission decreases upon increasing Yb^{3+} concentration but this does not lead to a strong increase in the Yb^{3+} emission. In all samples the Yb^{3+} emission around 980 nm is weak which shows that after energy transfer from Er^{3+} to Yb^{3+}, the Yb^{3+} luminescence is quenched, probably due to concentration quenching. The present results show that nonradiative relaxation from the $^4F_{7/2}$ level is too fast in $NaYF_4$ and DC of one visible into two NIR photons, as shown schematically in Fig. 1, is not possible with the Er^{3+}, Yb^{3+} couple. The energy difference between the $^4F_{7/2}$ level and the $^2H_{11/2}$ level is typically around 1300 cm^{-1}.[19–21] The maximum phonon energy in the $NaYF_4$ lattice is some 400 cm^{-1} which means that the energy gap can be bridged by ~3 phonons. Based on the energy gap law and experimental results a rule of thumb predicts that radiative decay and multiphonon relaxation can compete when the gap is five times the phonon energy.[8] For a smaller gap multiphonon relaxation dominates in agreement with the present observations. After fast multiphonon relaxation to the $^2H_{11/2}$ level, further relaxation to the $^4S_{3/2}$ level occurs. Emission from the $^4S_{3/2}$ level is observed to be partly quenched by Yb^{3+}. The quenching is however not very efficient. Even for Yb^{3+}-concentrations as high as 30% the remaining Er^{3+} ($^4S_{3/2}$) emission intensity is more than 1/3 of the intensity for the sample without Yb^{3+} even though almost every Er^{3+} ion has one or more nearest Yb^{3+}-neighbors. If we consider the energy level diagrams of Er^{3+} and Yb^{3+} we can understand the relatively low efficiency of the cross-relaxation process from the $^4S_{3/2}$ level of Er^{3+}. There are two possibilities for cross relaxation: Er^{3+} ($^4S_{3/2} \rightarrow {}^4I_{11/2}$) and Yb^{3+} ($^2F_{7/2} \rightarrow {}^2F_{5/2}$) or Er^{3+} ($^4S_{3/2} \rightarrow {}^4I_{13/2}$) and Yb^{3+} ($^2F_{7/2} \rightarrow {}^2F_{5/2}$). The energy for the transition on Yb^{3+} is around 10 200 cm^{-1}. There is a large energy mismatch for both cross-relaxation processes. The $^4S_{3/2} \rightarrow {}^4I_{11/2}$ energy difference is around 8500 cm^{-1} and the cross-relaxation process would involve a 1700 cm^{-1} thermal activation energy (four-phonon absorption). This will have a very low probability at 300 K. The energy mismatch for the second cross-relaxation process is similar but now the energy difference can be made up by emission of four phonons which is possible, albeit with low probability, also at low temperatures. The observed energy transfer from the $^4S_{3/2}$ state of Er^{3+} to Yb^{3+} is therefore assigned to a four-phonon assisted cross-relaxation process Er^{3+} ($^4S_{3/2} \rightarrow {}^4I_{13/2}$) and Yb^{3+} ($^2F_{7/2} \rightarrow {}^2F_{5/2}$).

Figure 4 shows the room temperature emission spectra for excitation in the Er^{3+} $^4G_{11/2}$ level (380 nm) for samples doped with 1% Er^{3+} and 0%, 5%, 10%, and 30% Yb^{3+}. The emission spectra show the same Er^{3+} emissions as for excitation in the $^4F_{7/2}$ level, but with different relative intensities. For the samples codoped with Yb^{3+} the $^2F_{5/2} \rightarrow {}^2F_{7/2}$ emission is observed, indicating that there is energy transfer from Er^{3+} to Yb^{3+}. Emission from the Er^{3+} $^4I_{11/2} \rightarrow {}^4I_{15/2}$ transition is observed at slightly shorter wavelength than the $^4F_{5/2} \rightarrow {}^4F_{7/2}$ transition of Yb^{3+}. Upon raising the Yb^{3+} concentra-

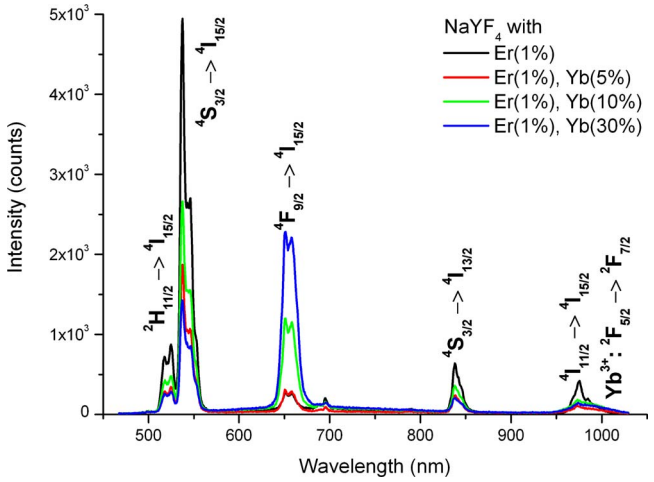

FIG. 4. (Color online) Room temperature emission spectra of $NaYF_4:Er^{3+}$ (1%) and Yb^{3+} (0%, 5%, 10%, and 30%) for excitation at 380 nm ($^4G_{11/2}$ level).

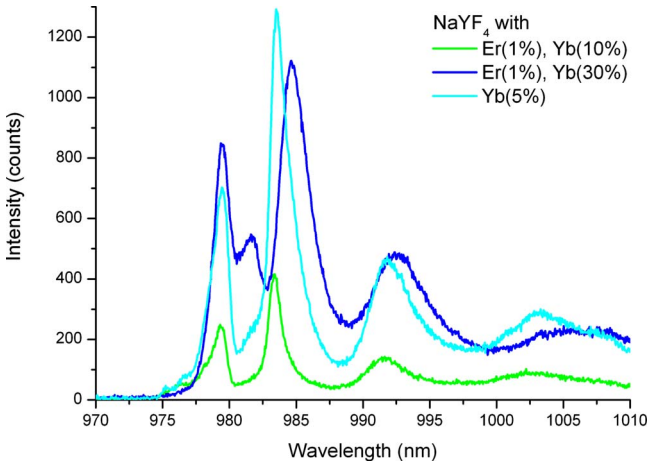

FIG. 6. (Color online) Emission spectra of the Yb^{3+} emission for $NaYF_4:Yb^{3+}$ (5%) (λ_x=954 nm), and $NaYF_4:Er^{3+}$ (1%) and Yb^{3+} (5% and 30%) (λ_x=380 nm) measured at 4 K.

tion, the $^4S_{3/2}$ emission intensity decreases. However, the intensity of emission from the $^4F_{9/2} \rightarrow {}^4I_{15/2}$ transition increases, contrary to the situation for excitation in the $^4F_{5/2}$ level where all Er^{3+} emission are observed to decrease upon raising the Yb^{3+} concentration (*vide supra*). The increase in the $^4F_{9/2}$ emission is explained by efficient cross relaxation between Er^{3+} and Yb^{3+}:Er^{3+} ($^4G_{11/2} \rightarrow {}^4F_{9/2}$) and Yb^{3+} ($^2F_{7/2} \rightarrow {}^2F_{5/2}$). The energy mismatch for this cross-relaxation process is small ($\sim$800 cm^{-1}) and can be accommodated by a two-phonon emission process. This process populates the $^2F_{9/2}$ level which yields the characteristic red emission of Er^{3+} around 660 nm (see Fig. 5). At the same time, Yb^{3+} is raised to the $^2F_{5/2}$ excited state. However, the $^2F_{5/2}$ emission from Yb^{3+} is weak. Both concentration quenching of the Yb^{3+} emission and the weak spectral response of the instrument in this spectral region contribute to the low emission intensity of Yb^{3+} observed in the spectrum. The efficiency of the cross-relaxation process can be estimated from the relative intensities of the $^4S_{3/2}$ emission and the $^4F_{9/2}$ emission. For the sample codoped with 30% Yb^{3+}, the $^4F_{9/2}$ emission dominates, indicating that more than half of the Er^{3+} show cross relaxation. Efficient cross relaxation from the $^4G_{11/2}$ level can be expected: the energy gap to the next lower $^4G_{9/2}$ level is typically 1800 cm^{-1} and requires five phonons to be bridged. As a result multiphonon relaxation will be slow and cross relaxation can compete with nonradiative multiphonon relaxation. The efficient cross relaxation from the $^4G_{11/2}$ level results in quantum cutting: absorption of a 380 nm photon gives the emission of a red 660 nm photon (from the $^4F_{9/2}$ level of Er^{3+}) and an infrared 980 nm photon (from the $^4F_{5/2}$ level of Yb^{3+}). For solar cell applications this quantum cutting process is not very useful as only a small part of the solar spectrum has wavelengths shorter than 380 nm.

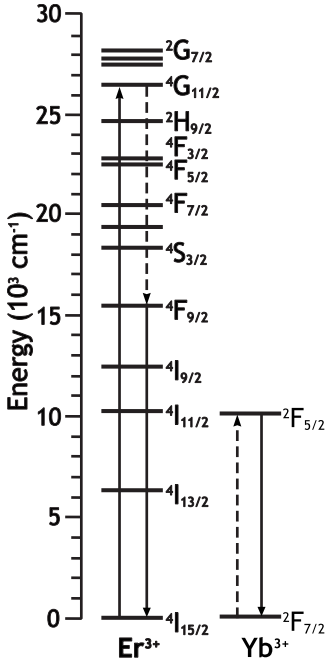

FIG. 5. Energy level scheme of the Er^{3+} and Yb^{3+} couple showing the DC mechanism starting from the $^4G_{11/2}$ level.

To study the Yb^{3+} emission spectra in more detail, higher resolution emission spectra were recorded in the spectral region around 1000 nm. In the spectra of the Yb^{3+} emission (Fig. 6) four peaks can be observed which can be explained by emission from the $^2F_{5/2}$ state to the four crystal field components of the $^2F_{7/2}$ ground state. The emission spectra for the three samples are very similar. A small shift in the positions of the peaks is observed upon raising the Yb^{3+} concentration, probably due to a small variation in the crystal field splitting resulting from the difference in ionic radius between Y^{3+} and Yb^{3+}. An extra peak around 982 nm is observed for the sample doped with 1% Er^{3+} and 30% Yb^{3+}. This is assigned to emission from an Yb^{3+}-trap level, possibly Yb^{3+} next to an O^{2-} ion on a F^- site. In the sample with 30% Yb^{3+} efficient energy migration over the Yb^{3+} sublattice will occur and the excitation energy can be trapped. In the samples doped with 5% or 10 % Yb^{3+} energy migration is not yet efficient (the concentrations are below the percolation point) and energy transfer to the Yb^{3+} traps is much less probable.

To gain further insight in the energy transfer processes

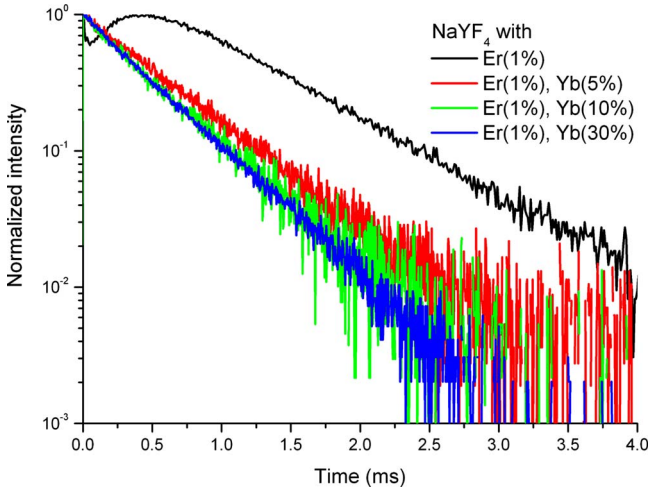

FIG. 7. (Color online) Luminescence decay curves for the $^4F_{9/2}$ emission in $NaYF_4:Er^{3+}$ 1%, codoped with 0%, 5%, 10%, or 30% Yb^{3+} measured at room temperature. The excitation wavelength is 380 nm (into the $^4G_{11/2}$ level) and the emission wavelength is 654 nm ($^4F_{9/2} \rightarrow {}^4I_{15/2}$).

between Er^{3+} and Yb^{3+}, luminescence decay curves were recorded. Luminescence decay curves of Er^{3+} emission upon excitation in the $^4G_{11/2}$ level of Er^{3+} are shown in Figs. 7 and 8. In Fig. 7 luminescence decay curves are shown for the $^4F_{9/2}$ emission in samples doped with 1% Er^{3+} and between 0% and 30% Yb^{3+}. In the sample without Yb^{3+}, there is a clear buildup in the first part of the decay of the $^4F_{9/2}$ emission due to slow multiphonon relaxation from the $^4G_{11/2}$ to $^4F_{9/2}$ level. The very fast initial decay observed before the buildup may be due to scattered laser light reaching the detector or to fast emission from Er^{3+} pairs where the $^4F_{9/2}$ level is populated by fast cross relaxation between neighboring Er^{3+} ions. The buildup disappears in the samples with Yb^{3+}, because the $^4F_{9/2}$ level is now efficiently populated by cross relaxation with neighboring Yb^{3+} ions [Er^{3+} ($^4G_{11/2} \rightarrow {}^4F_{9/2}$) and Yb^{3+} ($^2F_{7/2} \rightarrow {}^2F_{5/2}$)]. This observation provides additional evidence for the quantum cutting mechanism initiated by excitation in the $^4G_{11/2}$ level, as discussed

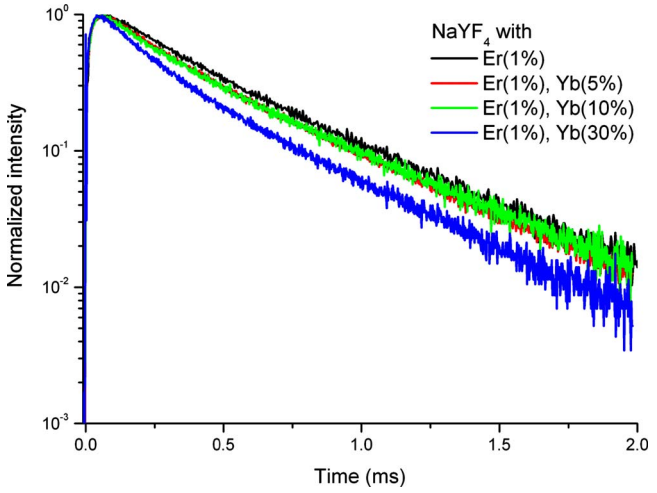

FIG. 8. (Color online) Luminescence decay curves for the $^4S_{3/2}$ emission in $NaYF_4:Er^{3+}$ 1%, codoped with 0%, 5%, 10%, or 30% Yb^{3+} measured at room temperature. The excitation wavelength is 380 nm (into the $^4G_{11/2}$ level) and the emission wavelength is 543 nm ($^4S_{3/2} \rightarrow {}^4I_{15/2}$).

in the previous section and shown in Fig. 5. The decay time of the $^4F_{9/2}$ emission depends only weakly on the Yb^{3+} concentration (560 μs for 5% Yb to 440 μs for 30% Yb) showing that energy transfer from the $^4F_{9/2}$ level of Er^{3+} to Yb^{3+} is inefficient. This is consistent with energy level scheme of Er^{3+}: there is no energy level 10 000 cm^{-1} below the $^4F_{9/2}$ level.

In Fig. 8 the decay curves of the $^4S_{3/2} \rightarrow {}^4I_{15/2}$ emission are shown upon excitation in the $^4G_{11/2}$ level. There is again a buildup in the signal, now due to relaxation from the $^4G_{11/2}$ level to the $^4S_{3/2}$ level. For the sample without Yb^{3+}, the $^4S_{3/2}$ emission decay is exponential with a decay time of 450 μs. As the Yb^{3+} concentration is increased, the decay of the $^4S_{3/2}$ emission becomes faster and nonexponential. This is due to energy transfer to neighboring Yb^{3+} ions. The nonexponential character of the decay is explained by the fact that each Er^{3+} donor has a different distribution of Yb^{3+} acceptors around it. In the long time regime the exponential ($\sim$450 μs) decay of Er^{3+} is observed for those Er^{3+} ions that do not have a nearest neighbor acceptor. Note that the shortening of the decay time is limited. This confirms that the energy transfer to Yb^{3+} is not efficient. The efficiency of energy transfer (the fraction of Er^{3+} that relaxes through energy transfer to Yb^{3+}, instead of through radiative decay) can be estimated from the integrals under the normalized decay curves.[12] From luminescence decay measurements energy transfer efficiencies for energy transfer from the Er^{3+} $^4S_{3/2}$ level to Yb^{3+} of 10%, 11%, and 28% can be estimated for the samples doped with 1% Er^{3+} and 5%, 10%, and 30% Yb^{3+}, respectively. Compared to the efficient energy transfer observed previously for the (Pr^{3+}, Yb^{3+}),[15,17] (Tm^{3+}, Yb^{3+}),[16] and (Tb^{3+}, Yb^{3+}) [14,22,23] couples, this efficiency is low and shows that the (Er^{3+}, Yb^{3+}) couple is unattractive as a DC couple in host lattices where the relaxation from the $^4F_{7/2}$ level to the $^4S_{3/2}$ level is fast. Only in host lattices with lower phonon energies (i.e., chloride and bromide host materials) DC from the $^4F_{7/2}$ level may compete with multiphonon relaxation and efficient quantum cutting may be achieved. At present, work on DC in the (Er^{3+}, Yb^{3+}) couple in chloride and bromide host materials is in progress.

IV. CONCLUSIONS

Luminescence spectra (excitation and emission) and luminescence decays curves have been recorded for $NaYF_4:Er^{3+}$ 1% codoped with 0%, 5%, 10%, or 30% Yb^{3+} to investigate the potential of the (Er^{3+}, Yb^{3+}) couple for DC. The results show that the desired DC process from the $^4F_{7/2}$ level (the inverse of the efficient UC process) has a very low efficiency due to fast multiphonon relaxation from the $^4F_{7/2}$ to the $^4S_{3/2}$ via the intermediate $^2H_{11/2}$ level. Based on the energy gap between the $^4F_{7/2}$ and the $^2H_{11/2}$ level (typically 1300 cm^{-1}) this is not unexpected in hosts with phonon energies over 250 cm^{-1}. In a host with a smaller phonon energies, viz. chloride or bromide host materials, emission from the $^4F_{7/2}$ level, and therefore DC, may be possible.

Upon excitation in the $^4G_{11/2}$ level (around 380 nm) efficient DC is observed. The increase in emission from the

Er^{3+} $^4F_{9/2}$ level upon raising the Yb^{3+} concentration, is due to a cross-relaxation process involving the $^4G_{11/2} \rightarrow {}^4F_{9/2}$ transition of Er^{3+} and the $^2F_{7/2} \rightarrow {}^2F_{5/2}$ transition of Yb^{3+}. Cross relaxation is followed by emission of a 650 nm photon from the Er^{3+} $^4F_{9/2}$ level and emission of a second photon (around 980 nm) by Yb^{3+}. This shows that quantum cutting of a 380 nm photon into a 650 nm photon and a 1000 nm photon is possible with the (Er^{3+}, Yb^{3+}) couple. Spectral conversion for solar cells using this DC scheme is not promising as the efficiency gain is limited due to the small fraction of the solar spectrum available in the wavelength region below 380 nm.

ACKNOWLEDGMENTS

This work is part of the Joint Solar Programme (JSP) of the Stichting voor Fundamenteel Onderzoek der Materie (FOM), which is supported financially by Nederlandse Organisatie voor Wetenschappelijk Onderzoek (NWO). The JSP is cofinanced by Gebied Chemische Wetenschappen of NWO and Stichting Shell Research. Financial support from the "Energie Onderzoek Subsidie" (EOS) program of SenterNovem, an agency of the "Ministerie van Economische Zaken" of The Netherlands, is gratefully acknowledged.

[1]W. Shockley and H. J. Queisser, J. Appl. Phys. **32**, 510 (1961).
[2]M. A. Green, K. Emery, Y. Hishikawa, and W. Warta, Prog. Photovoltaics **17**, 85 (2009).
[3]F. Auzel, Chem. Rev. (Washington, D.C.) **104**, 139 (2004).
[4]R. T. Wegh, H. Donker, K. D. Oskam, and A. Meijerink, Science **283**, 663 (1999).
[5]T. Trupke, M. A. Green, and P. Würfel, J. Appl. Phys. **92**, 1668 (2002).
[6]T. Trupke, M. A. Green, and P. Würfel, J. Appl. Phys. **92**, 4117 (2002).
[7]T. Trupke, A. Shalav, B. S. Richards, P. Würfel, and M. A. Green, Sol. Energy Mater. Sol. Cells **90**, 3327 (2006).
[8]J. F. Suyver, A. Aebischer, D. Biner, P. Gerner, J. Grimm, S. Heer, K. W. Krämer, C. Reinhard, and H. U. Güdel, Opt. Mater. (Amsterdam, Neth.) **27**, 1111 (2005).
[9]A. Shalav, B. S. Richards, T. Trupke, K. W. Krämer, and H. U. Güdel, Appl. Phys. Lett. **86**, 013505 (2005).
[10]K. D. Oskam, R. T. Wegh, H. Donker, E. V. D. van Loef, and A. Meijerink, J. Alloys Compd. **300–301**, 421 (2000).
[11]R.T. Wegh, E.V. D. van Loef, and A. Meijerink, J. Lumin. **90**, 111 (2000).
[12]P. Vergeer, T. J. H. Vlugt, M. H. F. Kox, M. I. den Hertog, J. P. J. M. van der Eerden, and A. Meijerink, Phys. Rev. B **71**, 014119 (2005).
[13]Q. Y. Zhang, G. F. Yang, and Z. H. Jiang, Appl. Phys. Lett. **91**, 051903 (2007).
[14]J. L. Yuan, X. Y. Zeng, J. T. Zhao, Z. J. Zhang, H. H. Chen, and X. X. Yang, J. Phys. D **41**, 105406 (2008).
[15]G. Lakshminarayana, H. Yang, S. Ye, Y. Liu, and J. Qiu, J. Mater. Res. **23**, 3090 (2008).
[16]G. Lakshminarayana, H. Yang, S. Ye, Y. Liu, and J. Qiu, J. Phys. D **41**, 175111 (2008).
[17]B. M. van der Ende, L. Aarts, and A. Meijerink, Adv. Mater. (Weinheim, Ger.) (in press).
[18]K. W. Krämer, D. Biner, G. Frei, H. U. Güdel, M. P. Hehlen, and S. R. Lüthi, Chem. Mater. **16**, 1244 (2004).
[19]X. Zhou, P. A. Tanner, and M. D. Foucher, J. Phys. Chem. C **111**, 683 (2007).
[20]A. M. Tkachuk, S. É. Ivanova, L. I. Isaenko, A. P. Yelisseyev, M. F. Joubert, Y. Guyot, and S. Payne, Opt. Spectrosc. **95**, 722 (2003).
[21]U. Hömmerich, E. E. Nyein, and S. B. Trivedi, J. Lumin. **113**, 100 (2005).
[22]Q. Y. Zhang, C. H. Yang, and Y. X. Pan, Appl. Phys. Lett. **90**, 021107 (2007).
[23]X. Y. Huang and Q. Y. Zhang, J. Appl. Phys. **105**, 053521 (2009).